

## New 3-D Chiral Framework of Indium with 1,3,5-Benzenetricarboxylate

Zhengzhong Lin, Feilong Jiang, Lian Chen, Daqiang Yuan, and Maochun Hong\*

State Key Laboratory of Structural Chemistry, Fujian Institute of Research on the Structure of Matter, Graduate School of the Chinese Academy of Sciences, Chinese Academy of Sciences, Fujian, Fuzhou, 350002 China

Received April 18, 2004

A new complex,  $[\text{In}_2(\mu\text{-OH})_2(\text{btc})_2]_n \cdot 2n\text{Hpy}$  (**1**) (btc = 1,3,5-benzenetricarboxylate; py = pyridine), is hydrothermally synthesized from the reaction of  $\text{InCl}_3$ ,  $\text{H}_3\text{btc}$ , and pyridine. Complex **1** crystallizes in the monoclinic  $P2_1$  space group [ $a = 7.3181(12)$  Å,  $b = 17.0195(23)$  Å,  $c = 10.5789(17)$  Å,  $\beta = 102.651(6)^\circ$ , and  $Z = 2$ ]. Indium(III) centers in **1** are bridged by btc ligands in various coordination modes to form the nonclose rings which are further interlinked along crystallographic  $a$ -axis and (011) plane to result in a nonpenetrated 3-D anionic framework growing as homochiral tunnels. Compound **1** is fully characterized by fluorescence spectroscopy, second harmonic generation measurement, infrared, and thermogravimetric analysis.

## Introduction

Porous chiral materials are recently attracting considerable interest on account of possible application in enantioselective separations.<sup>1</sup> Zeolites such as gallophosphates<sup>2</sup> and aluminophosphates<sup>3</sup> have been grown enantiomerically pure from resolved templates. A number of chiral open frameworks of phosphates<sup>4</sup> and of germinates<sup>5</sup> constructed from achiral starting materials have been reported. 1,3,5-Benzenetricarboxylic acid ( $\text{H}_3\text{btc}$ ) is currently an interesting tridentate ligand employed in the assembly of porous chiral frameworks<sup>6</sup> which exhibit a high degree of robustness toward solvent removal or exchange. The multidentate functionality

of  $\text{H}_3\text{btc}$  endows rigidity to the structure and therefore results in the robustness.<sup>7</sup> Porous chiral frameworks constructed from  $\text{H}_3\text{btc}$  and a transition metal are usually based on the interpenetration of two or four independent neutral network. Compared with the immense number of divalent metal–btc polymers,<sup>8,9</sup> reports on the polymers constructed from btc groups and trivalent metal are rarely documented.<sup>10</sup> However, the change of valence in metal centers may produce strikingly different structures. This idea prompts us to choose indium(III) as the metal ion and pyridine as an auxiliary ligand. Employing this strategy, we have successfully synthesized a novel indium(III) coordination polymer from btc,  $[\text{In}_2(\mu\text{-$

\* To whom correspondence should be addressed. E-mail: hmc@ms.fjirsm.ac.cn. Phone: 86-591-3792460. Fax: 86-591-3714946.

- (1) (a) Sundarababu, G.; Leibovitch, M.; Corbin, D. R.; Scheffer, J. R.; Ramamurthy, V. *Chem. Commun.* **1996**, 2159. (b) Page, P. C. B.; King, F.; Rochester, C. H.; Siddiqui, M. R. H.; Willock, D. J.; Hutchings, G. J. *J. Chem. Soc., Chem. Commun.* **1995**, 2409.
- (2) (a) Lin, C. H.; Wang, S. L. *Inorg. Chem.* **2001**, *40*, 2918. (b) Lii, K. H.; Chen, C. Y. *Inorg. Chem.* **2000**, *39*, 3374. (c) Stalder, S. M.; Wilkinson, A. P. *Chem. Mater.* **1997**, *9*, 2168.
- (3) Gray, M. J.; Jasper, J. D.; Wilkinson, A. P.; Hanson, J. C. *Chem. Mater.* **1997**, *9*, 976.
- (4) (a) Yilmaz, A.; Bu, X. H.; Kizilyalli, M.; Stucky, G. D. *Chem. Mater.* **2000**, *12*, 3243. (b) Simon, N.; Loiseau, T.; Ferey, G. *Solid State Sci.* **2000**, *2*, 389. (c) Bontchev, R. P.; Iliev, M. N.; Dezaneti, L. M.; Jacobson, A. J. *Solid State Sci.* **2001**, *3*, 133. (d) Boy, I.; Stowasser, F.; Schafer, G.; Kniep, R. *Chem.—Eur. J.* **2001**, *7*, 834. (f) Ayyappan, S.; Bu, X.; Cheetham, A. K.; Rao, C. N. R. *Chem. Mater.* **1998**, *10*, 3308.
- (5) Gier, T. E.; Bu, X.; Feng, P.; Stucky, G. D. *Nature* **1998**, *395*, 154.
- (6) (a) Prior, T. J.; Rosseinsky, M. J. *Inorg. Chem.* **2003**, *42*, 1564. (b) Kepert, C. J.; Prior, T. J.; Rosseinsky, M. J. *J. Am. Chem. Soc.* **2000**, *122*, 15158. (c) Kepert, C. J.; Rosseinsky, M. J. *Chem. Commun.* **1998**, 31.
- (7) Yaghi, O. M.; Davis, C. E.; Li, G. M.; Li, H. L. *J. Am. Chem. Soc.* **1997**, *119*, 2861.
- (8) (a) Plater, M. J.; Foreman, M. R. S. E.; Coronado, C. J.; Gómez-García, C. J.; Slawin, A. M. Z. *J. Chem. Soc., Dalton Trans.* **1999**, 4209. (b) Yaghi, O. M.; Li, H. L.; Groy, T. L. *J. Am. Chem. Soc.* **1996**, *118*, 9096. (c) Choi, H. J.; Suh, M. P. *J. Am. Chem. Soc.* **1998**, *120*, 10622. (d) Plater, M. J.; Howie, R. A.; Roberts, A. J. *Chem. Commun.* **1997**, 893. (e) Kepert, C. J.; Prior, T. J.; Rosseinsky, M. J. *J. Solid State Chem.* **2000**, *152*, 261. (f) Cheng, D. P.; Khan, M. A.; Houser, R. P. *Inorg. Chem.* **2001**, *40*, 6858. (g) Wu, G.; Shi, X.; Fang, Q. R.; Tian, G.; Wang, L. F.; Zhu, G. S.; Addison, A. W.; Wei, Y.; Qiu, S. L. *Inorg. Chem. Commun.* **2003**, *6*, 402. (h) Suh, M. P.; Ko, J. W.; Choi, H. J. *J. Am. Chem. Soc.* **2002**, *124*, 10976.
- (9) (a) Prior, T. J.; Rosseinsky, M. J. *Chem. Commun.* **2001**, 1222. (b) Chen, W.; Wang, J. Y.; Chen, C.; Yue, Q.; Yuan, H. M.; Chen, J. S.; Wang, S. N. *Inorg. Chem.* **2003**, *42*, 944. (c) Prior, T. J.; Rosseinsky, M. J. *Chem. Commun.* **2001**, 495. (d) Chui, S. S. Y.; Lo, S. M. F.; Charmant, J. P. H.; Orpen, A. G.; Williams, I. D. *Science* **1999**, *283*, 1148. (e) Prior, T. J.; Bradshaw, D.; Teat, S. J.; Rosseinsky, M. J. *Chem. Commun.* **2003**, 500.
- (10) (a) Daiguebonne, C.; Guilloa, O.; Gerault, Y.; Lecerf, A.; Boubekur, K. *Inorg. Chim. Acta* **1999**, *284*, 139. (b) Lin, Z. Z.; Luo, J. H.; Hong, M. C.; Wang, R. H.; Han, L.; Xu, Y.; Cao, R. *J. Solid State Chem.* **2004**, *177*, 2494–2498.

**Table 1.** Crystallographic and Structure Refinement Parameters for **1**

formula	C <sub>28</sub> N <sub>2</sub> O <sub>14</sub> In <sub>2</sub> H <sub>20</sub>	Z	2
fw	838.10	<i>d</i> <sub>calcd</sub> , g·cm <sup>-3</sup>	2.165
cryst syst	monoclinic	<i>T</i> , K	293
space group	<i>P</i> 2 <sub>1</sub>	λ(Mo Kα), Å	0.71073
<i>a</i> , Å	7.3181(12)	μ, mm <sup>-1</sup>	1.881
<i>b</i> , Å	17.0195(23)	<i>R</i> <sub>1</sub> ( <i>I</i> > 2σ( <i>I</i> )) <sup>a</sup>	0.0608
<i>c</i> , Å	10.5789(17)	w <i>R</i> <sub>2</sub> (all data) <sup>a</sup>	0.1436
β, deg	102.651(6)		

$$^a R_1 = \sum(|F_o| - |F_c|) / \sum|F_o|, wR_2 = [\sum w(F_o^2 - F_c^2)^2 / \sum w(F_o^2)^2]^{1/2}, w = 1/[\sigma^2(F_o^2) + (0.0497P)^2 + 11.5P], \text{ where } P = (F_o^2 + 2F_c^2)/3.$$

OH)<sub>2</sub>(btc)<sub>2</sub>]<sub>n</sub>·2*n*Hpy (**1**), which possesses a nonpenetrated 3-D structure with 1-D chiral tunnel. To the best of our knowledge, it is the first example of an indium(III)–btc polymer with an interesting three-dimensional framework.

## Experimental Section

**Materials and Analyses.** All reagents were of analytical grade and were used as obtained from commercial sources without further purification. IR (KBr pellets) spectra were recorded in the 400–4000 cm<sup>-1</sup> range using a Perkin-Elmer Spectrum One FTIR spectrometer. Elemental analyses were carried out on Elementar Vario EL III microanalyzer. Fluorescent data were collected on an Edinburgh FL-FS920 TCSPC system, and TG (thermal gravimetric) analysis was performed with a heating rate of 10 °C·min<sup>-1</sup> using a NETZSCH STA 449C simultaneous TG-DSC instrument.

**Preparation of [In<sub>2</sub>(btc)<sub>2</sub>(μ-OH)<sub>2</sub>]<sub>n</sub>·2*n*Hpy (**1**).** An aqueous mixture (4.0 mL) containing InCl<sub>3</sub> (26.0 mg, 0.12 mmol), H<sub>3</sub>btc (50.0 mg, 0.24 mmol), and pyridine (1.0 mL, 12.40 mmol) with the pH value around 6–7 was placed in a 30-mL Teflon-lined stainless steel autoclave, and the autoclave was sealed, heated to 160 °C under autogenous pressure for 85 h, and then cooled to room temperature at a rate of 6 °C/h. Light yellow crystalline product was filtered, washed with *N,N*-dimethylformamide, distilled water, and dried at ambient temperature to give 39 mg of complex **1** (yield 78% based on InCl<sub>3</sub>). Complex **1** is stable, and insoluble in water and most organic solvents. Anal. Calcd for C<sub>28</sub>N<sub>2</sub>O<sub>14</sub>·In<sub>2</sub>H<sub>20</sub>: C, 40.13; H, 2.41; N, 3.34%. Found: C, 39.66; H, 2.36; N, 3.40%.

**Crystallographic Studies.** Intensity data were collected on a Rigaku mercury CCD diffractometer with graphite-monochromated Mo Kα (λ = 0.71073 Å) radiation by using the ω–2θ scan method at room temperature. The structure was solved with direct methods and refined on *F*<sup>2</sup> with full-matrix least-squares methods using SHELXS-97 and SHELXL-97 programs, respectively.<sup>11</sup> All non-hydrogen atoms were refined anisotropically. All hydrogen atoms were added in the riding model and refined isotropically with C–H = 0.93 Å, N–H = 0.86 Å. Appropriate flack polarity parameter (0.03(6)) and SHG experiment<sup>12</sup> confirmed that a certain enantiomorph had been obtained in our initial structure determination. The crystallographic data are summarized in Table 1, and the selected bond lengths and bond angles are listed in Table 2.

## Results and Discussion

**Synthesis.** The formation of the indium(III)–btc complex was found to be extremely sensitive to the pH value of the

**Table 2.** Selected Bond Distances (Å) for **1**<sup>a</sup>

In(1)–O(13a)	2.011(9)	In(2)–O(5)	2.495(11)
In(1)–O(14)	2.080(8)	C(7)–O(1)	1.212(18)
In(1)–O(2b)	2.140(11)	C(7)–O(2)	1.296(18)
In(1)–O(3)	2.209(9)	C(8)–O(3)	1.244(17)
In(1)–O(9c)	2.330(9)	C(8)–O(4)	1.286(18)
In(1)–O(4)	2.359(10)	C(9)–O(5)	1.241(18)
In(1)–O(1b)	2.569(10)	C(9)–O(6)	1.244(17)
In(2)–O(10d)	2.126(9)	C(17)–O(7)	1.286(18)
In(2)–O(13)	2.145(9)	C(17)–O(8)	1.235(19)
In(2)–O(14e)	2.146(8)	C(18)–O(9)	1.274(17)
In(2)–O(6)	2.236(9)	C(18)–O(10)	1.295(18)
In(2)–O(7)	2.300(9)	C(19)–O(11)	1.273(17)
In(2)–O(8)	2.351(11)	C(19)–O(12)	1.250(17)

<sup>a</sup> Symmetry code: (a)  $-x, y + 1/2, -z + 1$ ; (b)  $-x - 1, y + 1/2, -z$ ; (c)  $x, y, z - 1$ ; (d)  $-x, y - 1/2, -z + 2$ ; (e)  $-x - 1, y - 1/2, -z + 1$ .

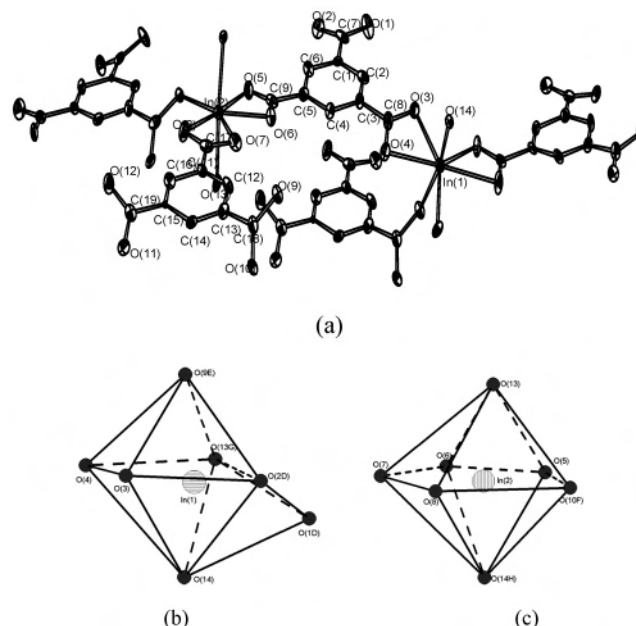


**Figure 1.** (a) ORTEP drawing (at 30% probability) of the coordination environment of indium atoms in **1**. (b) Diagram of the coordination configuration of In(1). (c) Diagram of the coordination configuration of In(2). Symmetry codes: (d)  $-x - 1, y + 1/2, -z$ ; (e)  $x, y, z - 1$ ; (f)  $-x, y - 1/2, -z + 2$ ; (g)  $-x, y + 1/2, -z + 1$ ; (h)  $-x - 1, y - 1/2, -z + 1$ . The symmetry codes are also applied in the text and later figures.

reaction mixture. Synthesis studies were carried out using pyridine as a basic reagent to adjust the pH value in the reaction system. With the pH value less than 3, a colorless crystalline complex, [In(btc)(H<sub>2</sub>O)]<sub>n</sub>·*n*H<sub>2</sub>O, was isolated from the reaction solution, and characterized by X-ray diffraction analysis which appears to be a 2-D layered structure. When the pH value was around 3–4, the mixture of [In(btc)(H<sub>2</sub>O)]<sub>n</sub>·*n*H<sub>2</sub>O and complex **1** formed. To ensure the high yield of complex **1**, much excessive pyridine was needed to adjust pH value around 6–7.

**Structural Description.** There are two indium(III) atoms, two btc ligands, and two μ-OH groups in an asymmetric unit of complex **1**. Each of two indium(III) atoms binds to five oxygen atoms from three btc ligands and two μ-OH groups to form a capped octahedron coordination geometry for In(1) or a slightly distorted pentagonal bipyramid for In(2), respectively (Figure 1a). In the In(1) center, O(1) from one carboxylate group of the btc ligand caps O(2D)–O(13G)–O(14), a triangular face of the octahedron, which exhibits a

- (11) (a) Sheldrick, G. M. *SHELXS97, Program for Crystal Structure Solution*; University of Göttingen: Göttingen, Germany, 1997. (b) Sheldrick, G. M. *SHELXL97, Program for Crystal Structure Refinement*; University of Göttingen: Göttingen, Germany, 1997.
- (12) Preliminary Kurtz powder second harmonic generation (SHG) measurement on complex **1** was done to confirm the chiral space group. Complex **1** exhibits a powder SHG efficiency of about 3 times as large as that of KDP. Its property indicates that **1** can be potentially applied in the field of nonlinear optics material.

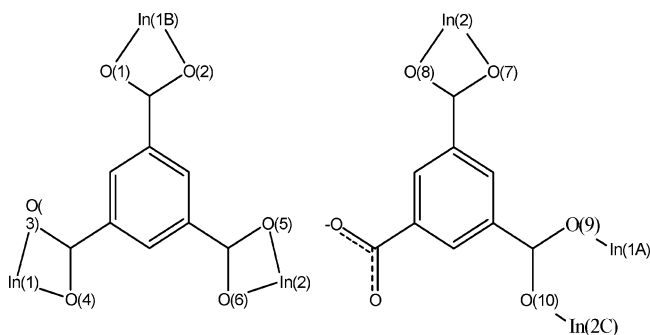


**Figure 2.** Scheme diagrams of btc groups: btc-A (left) and btc-B (right). Symmetry codes: (a)  $x, y, z + 1$ ; (b)  $-x - 1, y - 1/2, -z$ ; (c)  $-x, y + 1/2, -z + 2$ . The symmetry codes are also applied in the text and later figures.

distorted capped octahedron coordination (Figure 1b). In the In(2) center, the equatorial pentagonal plane is formed by five carboxylate oxygen atoms, O(5)–O(6)–O(7)–O(8)–O(10F), in which the five oxygen atoms and In(2) are almost coplanar with a mean deviation 0.13 Å, while two axial positions are occupied by O(13) and O(14H) from two  $\mu_2$ -OH groups with the O(13)–In(2)–O(14H) bond angle of  $170.4(3)^\circ$  (Figure 1c). The bond valences<sup>13</sup> of O(13) and O(14) are 1.263 and 1.135, respectively, indicating O(13) and O(14) are actually hydroxyl groups. The high coordination number conformation of indium ions in complex **1** is also observed in some In<sup>III</sup>–oxalate<sup>14</sup> and In<sup>III</sup>–terephthalate<sup>15</sup> complexes where each of the indium ions is coordinated by seven or eight oxygen atoms. The btc ligands with three carboxylate groups chelate to In(III) atoms in two different coordination modes. One btc ligand bonds metal atoms in chelating bidentate mode (btc-A) in which its three carboxylate groups are all deprotonated, and each of the carboxylate arms coordinates to a different In(III) atom as shown in Figure 2. The other btc ligand adopts a different coordination mode (btc-B), where one carboxylate arm of btc also bidentately coordinates an In(III) atom, while two oxygen atoms of another carboxylate arm link two In(III) atoms. The third carboxylate arm does not link to any metal ions (Figure 2). Since the amount of pyridine added is much in excess of that of H<sub>3</sub>btc during the preparation, and the two C–O bonds of carboxylate are almost equal (C(19)–O(11) = 1.273 Å and C(19)–O(12) = 1.250 Å), the deprotonation of the third carboxylate group is observed.

Indium(III) atoms are linked together by btc ligands in such a way to form a 3-D framework (Figure 3) possessing a 1-D tunnel along the [100] direction. Figure 4 shows a cross section layer of the framework, where nonclose rings, which are extended to spread to the whole layer, each consist of three indium(III) atoms, two btc-A groups, and one btc-B group. Rings can be divided into two categories because the proportion of In(1) and In(2) atoms in the rings is either 2 or  $1/2$ .

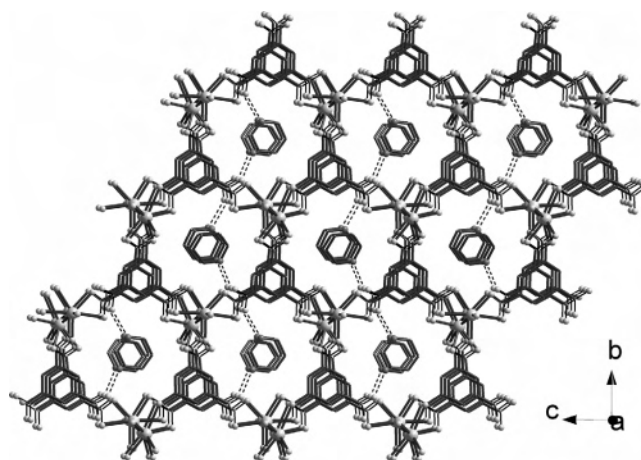


**Figure 3.** Packed structure of complex **1**, showing 1-D tunnels parallel to the [100] direction and the hydrogen bonds between pyridinium nitrogen atoms and uncoordinated carboxylate oxygen atoms.

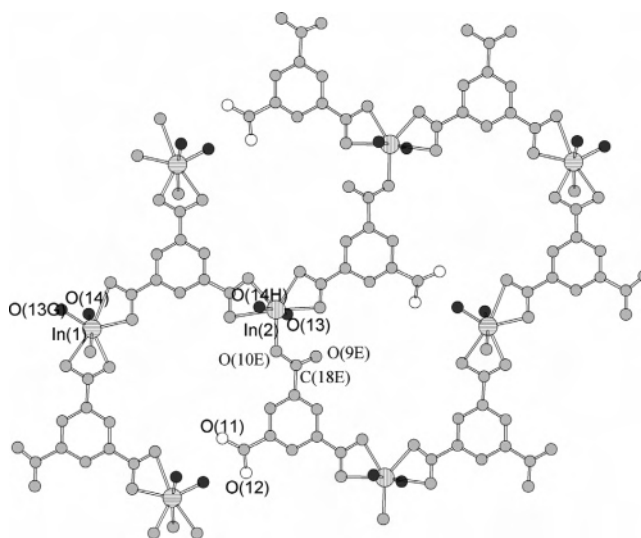


**Figure 4.** Cross section layer and pyridinium cations are not shown for clarity.

The rings are parallel each other and further link along the *a*-axis into 1-D chiral tunnels. The two neighboring rings are supported by three pillars, and the distance between two neighboring rings is about 3.8 Å. These pillars can also be divided into two categories according to their contents: one includes only a  $\mu$ -OH group, and the other can be regarded as combined pillars, each made up of another  $\mu$ -OH group and a carboxylate arm (O(9)–C(18)–O(10)) of btc-B. These two categories of pillars are arranged along the *a*-axis in an alternate way to interlink rings. The stacking mode of pillars creates infinite In–O–In–O– chains extended throughout the tunnels, as shown in Scheme 1. It is the inequivalent connections between inequivalent rings that result in the chirality of tunnels. The tunnels in **1** are of the same handedness. The rings of the pyridinium cations residing in the tunnels parallel to each other and the centroid–centroid distances are constrained to two values, 3.756(2) and 3.616(2) Å. When these extraframework species are not considered, the accessible volume within the crystal is calculated to be 31.8% by using the program PLATON.<sup>16,17</sup> Nitrogen atoms

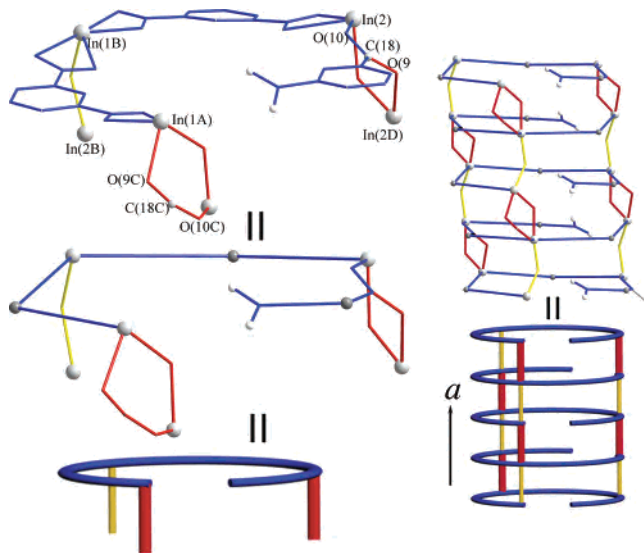
(13) Brese, N. E.; O'Keeffe, M. *Acta Crystallogr.* **1991**, B47, 192.

(14) (a) Audebrand, N.; Raite, S.; Louer, D. *Solid State Sci.* **2003**, 5, 783.

(b) Jeanneau, E.; Audebrand, N.; Louer, D. *J. Solid State Chem.* **2003**, 173, 387.

(15) Sun, J. Y.; Weng, L. H.; Zhou, Y. M.; Chen, J. X.; Chen, Z. X.; Liu, Z. C.; Zhao, D. Y. *Angew. Chem., Int. Ed.* **2002**, 41, 4471.

**Scheme 1.** Scheme Representation of Conceptual Diagram Showing a Chiral Tunnel<sup>a</sup>



<sup>a</sup> For clarity, only two carboxylate arms of btc in the ring, and a carboxylate arm (O(10C)–C(18C)–O(9C)) of btc-B in the pillar are shown.

form hydrogen bonds with the oxygen atoms from uncoordinated carboxylate groups ( $N(1)\cdots O(11) = 2.641 \text{ \AA}$  and  $N(2A)\cdots O(12) = 2.820 \text{ \AA}$ , symmetry code:  $A -x, y - 1/2, 2 - z$ ). The weak interactions in complex **1** also include the  $\pi$ – $\pi$  system found between the pyridinium cation rings and between btc benzene rings. The stacking environment for the benzene rings of btc is analogous to that of pyridine rings and also results in two  $\pi$ – $\pi$  systems with the centroid–centroid distances of  $3.720(3)$  and  $3.754(3) \text{ \AA}$ .

Two broad peaks of the IR spectrum centered at  $3620$  and  $3407 \text{ cm}^{-1}$  are mainly attributed to the  $\nu(\text{O}–\text{H})$  and  $\nu(\text{N}–\text{H})$  of the protonated nitrogen atoms' stretching vibrations. The absence of strong absorption bands in the area  $1720 \text{ cm}^{-1}$  confirms the fully deprotonation of the carboxylate groups of btc, which is consistent with the analysis of single X-ray diffraction. The bands between  $1605(\text{s})$  and  $1576(\text{s}) \text{ cm}^{-1}$  and between  $1450(\text{s})$  and  $1373(\text{s}) \text{ cm}^{-1}$  correspond to a bound carboxylate group  $\nu_{\text{asym}}$  and  $\nu_{\text{sym}}$  ( $\text{CO}_2\text{M}$ ), respectively, which indicates the carboxylate groups of the btc ligands coordinate to metal atoms in chelating bidentate mode. The peaks at  $1626(\text{s})$ ,  $1543(\text{s})$ ,  $1491(\text{s})$ , and  $1259(\text{m}) \text{ cm}^{-1}$  are associated with the pyridine ring stretching vibrations.

(16) (a) Spek, A. L. *Acta Crystallogr.* **1990**, *A46*, C34.

(17) Calculation was done by summing voxels more than  $1.2 \text{ \AA}$  away from the framework.

When illuminated with the wavelength of  $332 \text{ nm}$ , complex **1** displays two strong fluorescent emission bands centered at  $436$  and  $504 \text{ nm}$  ( $\text{fwhm} = 50 \text{ nm}$ ). It has been confirmed that  $\text{H}_3\text{btc}$  emits luminescence in the range  $370$ – $400 \text{ nm}$ ,<sup>18</sup> and some py containing ligands, such as  $4,4'$ -bipyridine, do not emit any luminescence in the range  $400$ – $800 \text{ nm}$ .<sup>19</sup> Thus, the emission of **1** might be related to a charge-transfer transition.<sup>20</sup> Thermogravimetric analysis of complex **1** was carried out in a flow of nitrogen atmosphere, and the framework of structure for **1** is still stable when temperature rises up to  $240 \text{ }^\circ\text{C}$ . Heating from  $250$  to  $515 \text{ }^\circ\text{C}$  results in complete collapse of the material of **1** with the simultaneous removal of py molecules and btc ligands. The residual weight  $48.0\%$  (calcd:  $48.9\%$ ) corresponds to  $\text{In}_2(\text{CO}_3)_3$ . On further heating, the product continues losing weight. At  $900 \text{ }^\circ\text{C}$ , the residue weighs  $41.34\%$ , which is also more than the expected value of  $33.1\%$  if the final material is  $\text{In}_2\text{O}_3$ . We consider the final product as the mixture of  $\text{In}_2(\text{CO}_3)_3$  and  $\text{In}_2\text{O}_3$ . In the X-ray powder diffraction pattern of final sintered product, strong peaks at  $\theta = 24.1^\circ$ ,  $33.0^\circ$ , and  $46.8^\circ$  that are associated with crystalline  $\text{In}_2\text{O}_3$  can be observed.<sup>21</sup> Some other major peaks are related to  $\text{In}_2(\text{CO}_3)_3$ . The preliminary attempts<sup>22</sup> to exchange the pyridinium cation guests with inorganic metal ions are unsuccessful, and we believe that the  $\pi$ – $\pi$  stacking in complex **1** may inhibit the diffusion of the pyridinium cations from the tunnels.

**Acknowledgment.** We acknowledge the support from National Natural Foundation of China (No. 20231020) and the Natural Science Foundation of Fujian Province.

**Supporting Information Available:** X-ray crystallographic files in CIF format, TG curve, fluorescent spectrum, and XRD pattern. This material is available free of charge via the Internet at <http://pubs.acs.org>.

IC0494962

- (18) (a) Fang, Q. R.; Zhu, G. S.; Shi, X.; Wu, G.; Tian, G.; Wang, R. W.; Qiu, S. L. *J. Solid State Chem.* **2004**, *177*, 1060. (b) Chen, W.; Wang, J. Y.; Chen, C.; Yue, Q.; Yuan, H. M.; Chen, J. S.; Wang, S. N. *Inorg. Chem.* **2003**, *42*, 944.
- (19) Tao, J.; Shi, J. X.; Tong, M. L.; Zhang, X. X.; Chen, X. M. *Inorg. Chem.* **2001**, *40*, 6328.
- (20) Dai, J. C.; Wu, X. T.; Cui, C. P.; Hu, S. M.; Du, W. X.; Wu, L. M.; Zhang, H. H.; Sun, R. Q. *Inorg. Chem.* **2002**, *41*, 1391.
- (21) JCPDS 22-336.
- (22) Ion exchange experiments are carried out by individually exposing solids of complex **1** to concentrated potassium, ammonium, calcium, and barium chloride salt solutions, respectively, at  $60 \text{ }^\circ\text{C}$  for 6 h. Since C, H, N contents of both original complex **1** and final products are almost the same, the pyridine molecules in complex **1** cannot be exchanged by the above-mentioned four inorganic ions.